Available online at www.sciencedirect.com

ScienceDirect

Mendeleev Commun., 2021, **31**, 315–318

Mendeleev Communications

Mn^{2+}-doped ZnS–CdS alloy nanocrystals for the photocatalytic hydrogen evolution reaction

Yurii A. Kabachii,[a] Sergey Yu. Kochev,*[a] Olga Yu. Antonova,[a] Sergey S. Abramchuk,[a] Alexandre S. Golub,[a] Artyom A. Astafiev,[b] Andrei N. Kostrov[b] and Victor A. Nadtochenko[b]

[a] *A. N. Nesmeyanov Institute of Organoelement Compounds, Russian Academy of Sciences, 119991 Moscow, Russian Federation. E-mail: kochew@ineos.ac.ru*

[b] *N. N. Semenov Federal Research Center for Chemical Physics, Russian Academy of Sciences, 119991 Moscow, Russian Federation*

DOI: 10.1016/j.mencom.2021.05.012

The effect of doping of the $Zn_xCd_{1-x}S$ (x = 0.37–0.50) alloy nanocrystals with Mn^{2+} ions on the rate and apparent quantum yield of the photocatalytic H_2 evolution catalyzed by this alloy has been investigated. It has been found that the ZnS shell significantly increases the lifetime of the Mn^{2+} excited state, which leads to the generation of 'hot' electrons and the two-photon photocatalytic reduction of hydrogen ions. An analysis of the characteristics of nanocrystals without a ZnS shell with similar excitation energies of the edge exciton revealed that the efficiency of the alloy doped with Mn^{2+} ions is 1.2–1.3 times higher due to an increase in the lifetime of photoinduced electron–hole pairs.

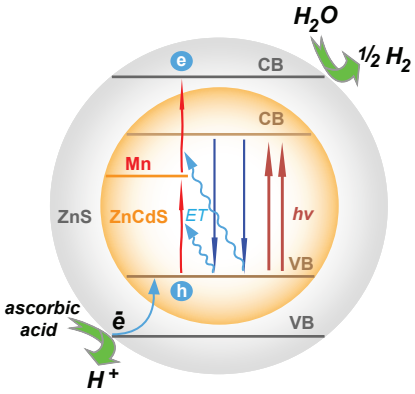

Keywords: hydrogen evolution reaction, nanocrystals, ZnS, Cd, Mn, alloy, hot electrons, lifetime, electron–hole pairs.

Semiconductor nanocrystals (NCs) doped with Mn^{2+} ions have attracted great interest in the last two decades due to their unique optical, electronic and opto-magnetic properties.[1,2] Such NCs are characterized by long-lived phosphorescence of Mn^{2+} ($^4T_1 \rightarrow {}^6A_1$) with a wavelength close to 600 nm, making this system extremely interesting for bioimaging applications.[3] Due to the long-lived excited state ($^4T_1$) of the Mn^{2+} ion, it can interact with an exciton generated by repeated excitation of NCs to generate high-energy, so-called 'hot' electrons with an increased electrochemical potential through the two-photon upconversion mechanism[4] (Figure 1). A series of experiments on photocurrent generation, photocatalytic reduction of methylene blue dye[5] and production of H_2 in aqueous dispersions[6] showed an increase in the photocatalytic activity of NCs doped with Mn^{2+} ions as compared to undoped ones. Considering the ever-growing worldwide interest in the conversion of solar energy into electrical or chemical energy, as well as the interest in the production of H_2 as a means of storing energy and environmentally friendly fuel,[7,8] the issue of the effect of doping with Mn^{2+} ions on the activity of semiconductor photocatalysts for producing hydrogen from water is of both theoretical and practical interest.

NCs of the Zn and Cd sulfide alloy with the composition $Zn_{0.5}Cd_{0.5}S$ are known[9–11] to exhibit higher catalytic activity in the photocatalytic production of H_2 than NCs of each of the components (ZnS and CdS) separately. Alloy $Zn_xCd_{1-x}S$ (x ~ 0.5) is a suitable system for doping with Mn^{2+} ions because the Mn^{2+} ion has an intermediate radius between the radii of Zn^{2+} and Cd^{2+} ions, the crystal lattice of the alloy retains well manganese atoms, and the alloy itself has high thermal and chemical resistance.[12]

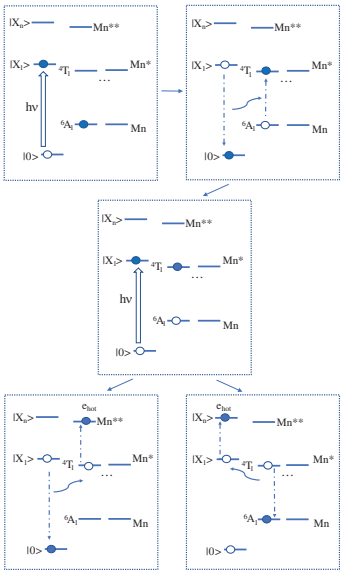

Figure 1 Simplified diagram showing possible pathways for the formation of high-energy 'hot' electrons (e_{hot}) in Mn^{2+}-doped ZnS–CdS alloy NCs through the two-photon upconversion mechanism.

In this work, we investigated the effect of doping with Mn^{2+} ions on the photocatalytic activity of the $Zn_xCd_{1-x}S$

Table 1 Composition and characteristics of NCs as photocatalysts in the hydrogen evolution reaction.

Sample	Composition	x	Mn content (mol%)	NC size/ nm[b]	EE/ eV[c]	HR/mmol h^{-1} g^{-1}		Apparent QY (%)
						Lamp (270–800 nm)	Laser (445 nm)[f]	
1	$Zn_xCd_{1-x}S$	0.37	0	5.2±0.8	2.76	101±3	1620±110	2.37±0.02
2	$Zn_xCd_{1-x}S$	0.5	0	5.7±0.9	2.86	233±9	419±4	1.49±0.01
3	$Mn:Zn_xCd_{1-x}S$	0.49	0.47	4.4±1.2	2.88	272±4	556±16	1.75±0.05
4	$Mn:Zn_xCd_{1-x}S/ZnS$	0.48[a]	0.60	7.6±0.9[d]	3.08	9.57±0.12	0.61±0.02	<0.01
5	$Zn_xCd_{1-x}S/ZnS$	0.82	0	9.5±1.1	3.00	34.7±0.2	1.9±0.1	<0.01
6	ZnS	1.0	0	6.0±1.2	3.88	0.24±0.01	<0.01	<0.01
7	ZnS/CdS	0.44	0	5.5±0.9[e]	3.06	93.7±1.1	1050±10	1.83±0.02

[a] Zn fraction in the NC core. [b] According to the TEM data. [c] The excitation energy of edge exciton. The maxima were found by differentiating the light absorption curves. [d] Shell thickness of 1.9 nm, core size of 3.8 ± 0.9 nm. [e] Shell thickness of 0.7 nm, core size of 4.1 ± 0.9 nm. [f] The luminous flux density was 3.40 W cm^{-2}.

(x = 0.37–0.50) alloy NCs, coated and uncoated with the ZnS shell, in photocatalytic hydrogen evolution. We prepared the NCs by thermal decomposition of Zn and Cd oleates and Mn stearate in an organic solvent at temperatures of 280–305 °C in the presence of molecular S.† Mn stearate is less reactive than other precursors and may react incompletely. Moreover, although the crystal lattice parameters of MnS are close to those of the alloy, the alloy doped with Mn^{2+} ions is still not a thermodynamically stable structure. A relatively large amount of Mn stearate had to be used to prevent the formation of undoped NCs. The molar fraction of manganese in the total amount of metals in the precursor mixture was about 0.1. We carried out photocatalytic tests of NCs in aqueous dispersions obtained by coating NCs with macromolecules of an amphiphilic cationic polyelectrolyte.[13] The light sources were a metal-halogen lamp with a radiation spectrum close to sunlight (λ = 270–800 nm, photon energy 1.6–4.6 eV) and an LED laser (λ = 445 nm, photon energy 2.79 eV). To eliminate the co-catalytic effect of manganese, 1% Pt co-catalyst, which is most effective in an acidic medium, was used.[13,†] The photocatalysis efficiency was characterized by the hydrogen evolution rate (HR) and the apparent quantum yield (QY). The composition and properties of the NCs are presented in Table 1.

According to powder X-ray diffraction data [Figure S2(*a*)], the structure of sample 3 doped with Mn^{2+} ions is best described by a hexagonal phase with parameters a and c, taking an intermediate value between those in the hexagonal phases of ZnS and CdS, with a small inclusion of the cubic phases of ZnS and CdS (Table S1).† These parameters correspond to the previously investigated ZnS–CdS alloy.[14] The structure of sample 4 is well described by a combination of only hexagonal (75%) and cubic (25%) ZnS modifications.† The presence of the mixed ZnS–CdS phase is not visible.† These results are consistent with the previous report,[15] in which only reflections from the ZnS shell were present in the diffraction pattern of the CdSe/ZnS core–shell nanocrystals, while the diffraction features of the core phase were not observed. The very low total content of Mn impurities in the $Zn_xCd_{1-x}S$ NCs, shown in Table 1, did not allow us to reliably confirm, using simulation, its effect on the formation of the entire crystal system of such a multicomponent sample since this effect (if any) should also be insignificant.

Figure 2 shows typical absorption and photoluminescence (PL) spectra of NCs, undoped (sample 2) [Figure 2(*a*)] and doped with Mn^{2+} ions (sample 3) [Figure 2(*b*)], as dispersions in hexane and water. The emission band at about 440 nm refers to the luminescence of an edge exciton, the QY of which is determined by the competition between the radiative optical transition and the capture of an electron, hole or both by trap states of different nature.[16–18] The band around ~590 nm is due to the PL of Mn^{2+} ions. The excitation spectrum of the Mn^{2+} luminescence band [Figure 2(*b*), curve *5*] coincides with the exciton absorption band of ZnS–CdS [Figure 2(*b*), curve *3*], indicating that the excitation of Mn^{2+} occurs due to nonradiative energy transfer from the excited exciton state of the NC to the d^5 levels of Mn^{2+}. As one can see from Figure 2, the aqueous medium significantly reduced the emission of intrinsic excitons in NCs containing no manganese ions [Figure 2(*a*), curves *1* and *2*], but less strongly influenced the emission of Mn^{2+} ions [Figure 2(*b*), curves *1* and *2*]. The luminescence yield of the edge exciton upon excitation at a wavelength of 360 nm decreased by 24 times upon transfer of NCs from hexane to water. The luminescence QY of the ~590 nm band upon excitation at 360 nm was 60% in hexane and 30% in water. Apparently, the decrease in the NC edge exciton luminescence in water can be associated with the formation of additional quenching centers, *i.e.*, traps. The review[18] discusses various trapping centers for semiconductor NCs in water, which usually arise due to surface defects. The relatively weaker effect of water on the Mn^{2+} luminescence indicates that the quenching of edge excitons by traps does not suppress the competitive energy transfer to the Mn^{2+} d^5 levels and, at the same time, the traps do not act as efficient quenchers of excited Mn^{2+}.

Figure 3 shows the kinetic curves of PL decay caused by the relaxation of the alloy edge excitons and by Mn^{2+} ions in NC samples 3 and 4. One can see that the manganese PL at 600 nm and its excited state lifetime last much longer than the alloy exciton PL. Coating doped NCs with a shell made of a wide-gap semiconductor ZnS[19] significantly reduces the decay of Mn^{2+} luminescence, which indicates that the decay is also affected by charge acceptors on the NC surface.

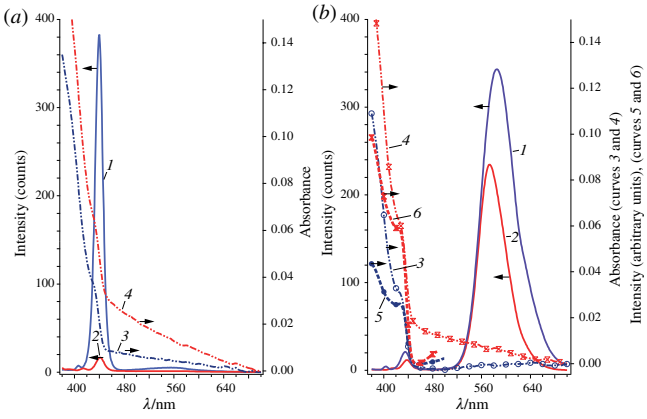

Figure 2 Absorption and emission spectra of NCs, (*a*) undoped (sample 2) and (*b*) doped with Mn^{2+} ions (sample 3): luminescence spectra at an excitation wavelength of 360 nm in (*1*) hexane and (*2*) water, absorption spectra in (*3*) hexane and (*4*) water and luminescence excitation spectra at a wavelength of 585 nm in (*5*) hexane and (*6*) water.

† For details, see Online Supplementary Materials.

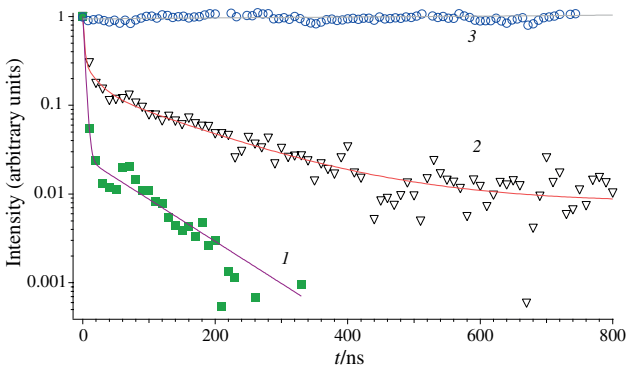

Figure 3 Luminescence decay curves of NCs doped with Mn^{2+} ions in (*1*) sample 3 at a wavelength of 440 nm (edge exciton PL), (*2*) sample 3 at a wavelength of 600 nm (Mn^{2+} PL) and (*3*) sample 4 at a wavelength of 600 nm (Mn^{2+} PL).

As shown above, ZnS-coated NCs exhibit the lowest decay of the Mn^{2+} PL and, accordingly, the highest steady-state concentration of manganese ions in the excited state. Therefore, their interaction with the second exciton and the generation of high-energy electron–hole pairs are most probable here. As shown by the study of photocatalytic activity, NCs coated with the ZnS shell (see Table 1, samples 4 and 5) demonstrate significantly lower activity compared to NCs without coating (samples 1–3) due to an increase in the energy required for electrons to enter the conduction band (CB) of the shell. The HR measurement results for alloy NCs coated with the ZnS shell and doped (sample 4) or undoped (sample 5) with Mn^{2+} ions at various luminous flux densities (F) are presented in Table S2[†] and Figure 4.

As one can see in Figure 4, HR dependence on the illumination intensity differs for undoped and doped NCs. Although both samples demonstrate an increase in HR with increasing illumination intensity, HR slows down for undoped NCs and accelerates for doped NCs starting from a certain F value (about 0.28 W cm^{-2} or 6.2×10^{17} photons cm^{-2} s^{-1}). Moreover, the straight line plotted in this section in logarithmic coordinates gives the degree of HR dependence on F equal to 2.08±0.09. The second order of the dependence of the reaction rate on F indicates a two-photon process of photocatalytic reduction of hydrogen atoms. Apparently, this fact can be considered evidence of the two-photon generation of high-energy ('hot') electrons in the NC core, as suggested in Figure 1. The absorption cross-section of NCs lies in the range of ~10^{-15}–10^{-14} cm^2 in order of magnitude,[20–23] and the photon absorption frequency should be in the range from ~6×10^2 to 6×10^3 s^{-1} at this flux density.

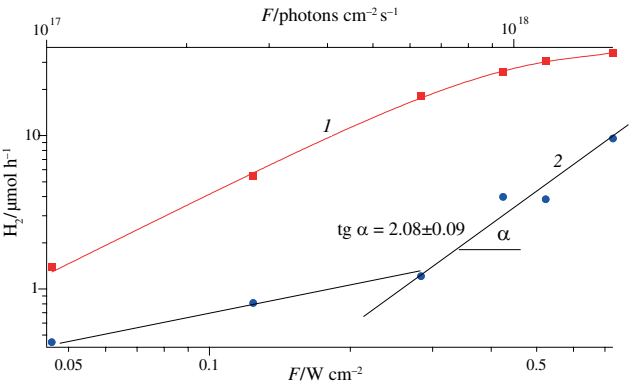

Figure 4 Plots of the H_2 evolution rate *vs.* luminous flux F for (*1*) NCs without manganese atoms (sample 5) and (*2*) NCs doped with Mn^{2+} (sample 4). The plot in logarithmic coordinates is approximated by a straight line with a slope of 2.08±0.09.

Note that, under the experimental conditions, the generation of electrons reducing hydrogen atoms occurred in the NC core, and the ZnS shell practically did not participate in it. This conclusion follows from the low HR value obtained upon illumination of ZnS NC (sample 6) with the maximum intensity of 0.728 W cm^{-2}, which is 40 and 140 times lower than the HR values for doped and undoped alloy NCs, respectively. Therefore, a slight decrease in the rate for undoped NCs is presumably associated with an increase in the probability of relaxation of photoinduced charges in the NC core under high illumination conditions and their high concentration as a consequence. In the case of doped NCs, the increase in HR occurs because the energy of 'hot' electrons becomes sufficient to transition to a higher located CB of the ZnS shell and reduce hydrogen ions in a high yield due to an increase in the electrochemical potential. Thus, the alloy NCs doped with Mn^{2+} ions and coated with the ZnS shell can be considered a converter of photoinduced low-energy electron–hole pairs into high-energy ones.

It is noteworthy that, on average, the HR of undoped NCs is higher than that of doped NCs. It can be assumed that, since the energy of photoinduced charges in the NC cores is insufficient for their access to the ZnS shell surface, a significant part of them is spent on the excitation of Mn^{2+} ions in doped NCs, which causes PL in the region of 600 nm. The intrinsic PL of the undoped alloy in the 440 nm region requires much higher excitation energy.

To compare the photocatalytic activity of the alloy and CdS, we synthesized NCs with the ZnS/CdS core/shell structure (see Table 1, sample 7). As expected, the CB state of the NC material depended on the alloy composition. This state can be characterized by the excitation energy of the edge exciton (see Table 1, EE) and is known[24] to be somewhat less than the CB bottom by the value of the exciton binding energy. The activity of $Zn_xCd_{1-x}S$ alloy NCs with an EE value close to that of sample 7 (*i.e.*, the CB bottom) and sample 1 ($x = 0.37$), measured with a narrow-band light source (laser), was found to be 1.5 and 1.3 times higher than that of ZnS/CdS NCs in terms of the HR and QY values, respectively. At the same time, the activity measured with a broadband light source (lamp) was practically the same. The laser radiation quantum energy (2.79 eV) exceeded in this case the excitation energy of excitons in both NCs. Interestingly, the HR and QY values of ZnS/CdS NCs measured under laser illumination were close to those of CdS NCs that we studied earlier under the same conditions (996 mmol h^{-1} g^{-1} and 1.85%, respectively).[13] In this case, the thickness of the CdS layer in ZnS/CdS was about 0.7 nm. This result confirms the conclusion about the participation of photoinduced electrons of a thin surface layer of the photocatalyst[11] in photocatalysis.

An increase in the ZnS content in the alloy to $x = 0.5$ (sample 2) increased EE to a value of 2.86 eV, exceeding the laser quantum energy, which sharply reduced the activity 3.9 and 1.6 times according to HR and QY data, respectively, compared with sample 1. On the contrary, the activity of sample 2 increased by more than 2 times when illuminated by a lamp. The reason for this change in the NC activity is a decrease in the efficiency of the generation of electron–hole pairs caused by an increase in EE to a value exceeding the energy of a laser radiation quantum. However, the absorption of the short-wavelength part of the lamp light increases their generation efficiency by reducing the probability of the formation of excited states, the relaxation of which can lead to a loss of absorbed energy due to PL.

The similarity of the EE values of alloy NCs doped with Mn^{2+} ions (sample 3) and undoped (sample 2), which do not contain a ZnS shell, makes it possible to compare their photocatalytic activity. Both with the lamp and the laser, the HR and QY values

of doped NCs were 1.2 and 1.3 times higher than those of undoped NCs, respectively.

Comparing the PL decay times of Mn^{2+} ions in alloy NCs without a shell and with a ZnS shell (see Figure 3) shows that the concentration of photoexcited Mn^{2+} ions in the former is more than an order of magnitude lower than in the latter. Therefore, based on the experimental results presented in Figure 4, it can be concluded that the two-photon generation of high-energy electrons in alloy NCs without a shell requires luminous flux density higher than 3 W cm^{-2}. As a result, a slight improvement in the photocatalytic characteristics of doped NCs is most likely associated only with the partial generation of 'hot' electrons. In this case, the Mn^{2+} ions, photoexcited to the long-lived $^4T_1$ state, can play the role of a buffer that accumulates the energy of excess excitons and thereby coordinating the flows of photoinduced charges and charges consumed for the electrochemical reduction of H_2O, since the time parameters of these two processes (physical and chemical) differ. In practice, this should lead to an increase in the lifetime of photoinduced electron–hole pairs.

Thus, the analysis of NCs of $Zn_xCd_{1-x}S$ alloys, doped and undoped with Mn^{2+} ions, in the ZnS shell showed that the shell significantly increases the lifetime of the excited state of Mn^{2+}, which leads to the generation of 'hot' electrons and two-photon photocatalytic reduction of hydrogen atoms at luminous flux densities exceeding 0.28 W cm^{-2} (6.2×10^{17} photons cm^{-2} s^{-1}). Comparison of the photocatalytic characteristics of NCs of the alloys, doped and undoped with Mn^{2+} ions, without the ZnS shell with similar excitation energies of the edge exciton showed a somewhat (1.2 and 1.3 times in terms of HR and QY, respectively) higher efficiency of the former due to an increase in the lifetime of photoinduced electron–hole pairs.

This work was supported by the Russian Science Foundation (grant no. 17-13-01506). X-ray diffraction studies were performed with the financial support from the Ministry of Science and Higher Education of the Russian Federation using the equipment of Center for molecular composition studies of INEOS RAS.

Online Supplementary Materials

Supplementary data associated with this article can be found in the online version at doi: 10.1016/j.mencom.2021.05.012.

References

1 D. J. Norris, A. L. Efros and S. C. Erwin, *Science*, 2008, **319**, 1776.
2 R. Beaulac, P. I. Archer, J. van Rijssel, A. Meijerink and D. R. Gamelin, *Nano Lett.*, 2008, **8**, 2949.
3 M. Singhal, J. K. Sharma, H. C. Jeon, T. W. Kang and S. Kumar, *Adv. Appl. Ceram.*, 2019, **118**, 321.
4 D. Parobek, T. Qiao and D. H. Son, *J. Chem. Phys.*, 2019, **151**, 120901.
5 H.-Y. Chen, T.-Y. Chen, E. Berdugo, Y. Park, K. Lovering and D. H. Son, *J. Phys. Chem. C*, 2011, **115**, 11407.
6 Y. Dong, J. Choi, H.-K. Jeong and D. H. Son, *J. Am. Chem. Soc.*, 2015, **137**, 5549.
7 *Hydrogen as a Future Energy Carrier*, eds. A. Züttel, A. Borgschulte and L. Schlapbach, Wiley-VCH, Weinheim, 2008.
8 Q. Wang and K. Domen, *Chem. Rev.*, 2020, **120**, 919.
9 H. Wang, Y. Li, D. Shu, X. Chen, X. Liu, X. Wang, J. Zhang and H. Wang, *Int. J. Energy Res.*, 2016, **40**,1280.
10 C.-C. Shen, Y.-N. Liu, X. Zhou, H.-L. Guo, Z.-W. Zhao, K. Liang and A.-W. Xu, *Catal. Sci. Technol.*, 2017, **7**, 961.
11 Q. Li, H. Meng, P. Zhou, Y. Zheng, J. Wang, J. Yu and J. R. Gong, *ACS Catal.*, 2013, **3**, 882.
12 A. Nag, S. Chakraborty and D. D. Sarma, *J. Am. Chem. Soc.*, 2008, **130**, 10605.
13 Yu. A. Kabachii, A. S. Golub', A. S. Goloveshkin, S. S. Abramchuk, A. V. Shapovalov, M. I. Buzin, P. M. Valetskii and S. Yu. Kochev, *Russ. Chem. Bull., Int. Ed.*, 2014, **63**, 2355 (*Izv. Akad. Nauk, Ser. Khim.*, 2014, 2335).
14 Y.-T. Nien, P.-W. Chen and I.-G. Chen, *J. Alloys Compd.*, 2008, **462**, 398.
15 A. Gulin, A. Shakhov, A. Vasin, A. Astafiev, O. Antonova, S. Kochev, Y. Kabachii, A. Golub and V. Nadtochenko, *Appl. Surf. Sci.*, 2019, **481,** 144.
16 M. Jones, S. S. Lo and G. D. Scholes, *Proc. Natl. Acad. Sci. U. S. A.*, 2009, **106,** 3011.
17 A. L. Stroyuk, V. M. Dzhagan, S. Ya. Kuchmii, M. Ya. Valakh, D. R. T. Zahn and C. von Borczyskowski, *Theor. Exp. Chem.*, 2007, **43,** 297 (*Teor. Eksp. Khim.*, 2007, **43**, 275).
18 L. Jing, S. V. Kershaw, Y. Li, X. Huang, Y. Li, A. L. Rogach and M. Gao, *Chem. Rev.*, 2016, **116,** 10623.
19 S. I. Sadovnikov, *Russ. Chem. Rev.*, 2019, **88**, 571.
20 C. A. Leatherdale, W.-K. Woo, F. V. Mikulec and M. G. Bawendi, *J. Phys. Chem. B*, 2002, **106**, 7619.
21 T. Ihara and Y. Kanemitsu, *Phys. Rev. B*, 2015, **92**, 155311.
22 J. Nanda, S. A. Ivanov, H. Htoon, I. Bezel, A. Piryatinski, S. Tretiak and V. I. Klimov, *J. Appl. Phys.*, 2006, **99**, 034309.
23 P. Yu, M. C. Beard, R. J. Ellingson, S. Ferrere, C. Curtis, J. Drexler, F. Luiszer and A. J. Nozik, *J. Phys. Chem. B*, 2005, **109**, 7084.
24 D. A. Wheeler and J. Z. Zhang, *Adv. Mater.*, 2013, **25,** 2878.

Received: 30th November 2020; Com. 20/6381